

Computation of iron and eddy-current losses in IPM motors depending on the field weakening angle and current waveform

Thomas Finken and Kay Hameyer

Institute of Electrical Machines, RWTH Aachen University
Schinkelstr. 4, 52056 Aachen, Germany; Email: thomas.finken@iem.rwth-aachen.de

Abstract –Due to the limited space availability and the high demand on power density and efficiency, the permanent magnet synchronous machine is suitable for application in parallel hybrid electric vehicles. The desired reduction of the vehicle’s fuel consumption requires a good efficiency, and thus low losses. Since the machine is operated over a wide range of operation points, the losses must be calculated depending on different values of the current, the field-weakening angle and the rotational speed. Since the harmonic content has a significant effect on losses, the effect of block-shaped currents and real current forms of PWM-fed machines are also studied in this paper.

Introduction

Due to the limited space availability and high demands on power density and overall efficiency, the permanent magnet synchronous machine (PMSM) is the most applied machine type for parallel hybrid electric vehicles (HEV). The desired reduction of fuel consumption implies a good overall efficiency and thus losses as low as possible. The integrity of the permanent magnets is a crucial element for the definition of the overload capacity and the thermal limits of the machine. As the resistance of the magnets against demagnetization decreases with increasing temperature, the allowed temperature increase in the machine is strictly limited. Integration into the drive train and the close positioning of the combustion engine worsens this problem. The losses in the machine should therefore be calculated as early as possible in the design process. Efficiency maps and loss maps over the operation range of the machine must be generated and used to optimize the design and determine the thermal operation limits. The machine is operated according to the vehicle’s driving cycle, over a large speed- and torque range, Losses must therefore be calculated for different current values, field-weakening angles and rotational speeds. To obtain high dynamic performances, increase the speed range and improve the torque at high speeds, the machine can be operated in the over-modulated region [1]-[2], or block-shaped voltages [3]-[4] can be applied. The resulting currents contain higher harmonics. Because the harmonic content greatly affects the iron losses, as well as on the eddy-current losses in the permanent magnets, its effect is also studied in this paper.

The electrical machine

The electrical machine under analysis is an eight-pole internal permanent magnet synchronous machine (IPMSM) with concentrated windings. The machine's cross-section and the rated data are depicted in Fig.1 and Table I.

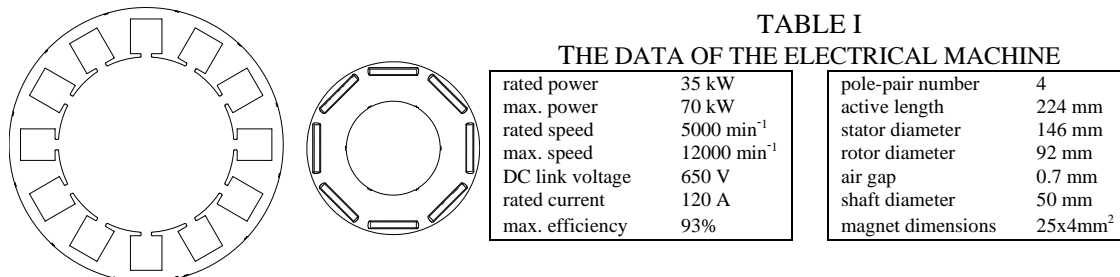


Fig.1. Cross-section of the electrical machine.

This machine was designed in the context of the BMWi¹ cooperative project *Europa Hybrid* for a parallel hybrid electric vehicle as described in [5].

The torque of a synchronous machine can be determined, with the pole-pair number p , the mechanical speed ω , the induced voltage U_p , the current I_q and reactance X_q in quadrature axis and the current I_d and reactance X_d in direct axis, by:

$$T = \frac{3p}{\omega} [U_p + I_d \cdot (X_q - X_d)] \cdot I_q \quad (1)$$

The currents $I_q = I \cos \psi$ and $I_d = I \sin \psi$ depend on the field-weakening angle ψ , see Fig.2(a). Due to the saliency of the IPMSM ($X_q > X_d$), there is an optimum angle ψ_{opt} offering the highest torque at a certain current (see Fig.2(b)). Up to the nominal speed the machine is operated with $\psi = \psi_{opt}$ (maximum-torque-per-ampere control, MTPA). Above nominal speed, in the field-weakening range, the negative current in direct axis I_d must be increased ($\psi < \psi_{opt}$) to weaken the rotor field, lower the induced voltage and limit the terminal voltage U_s to the maximum voltage (maximum-torque-per-voltage control, MTPV), which in turn is limited by the dc-link voltage and the battery voltage respectively.

Since the machine is operated over a wide speed- and torque range during the vehicle's driving cycle, the load current and the field-weakening angle change permanently. Thus, a loss calculation depending on the load current and the field-weakening angle is necessary to predict the machine's efficiency and thermal limits, especially in the speed range of field weakening and in the range of overload operation.

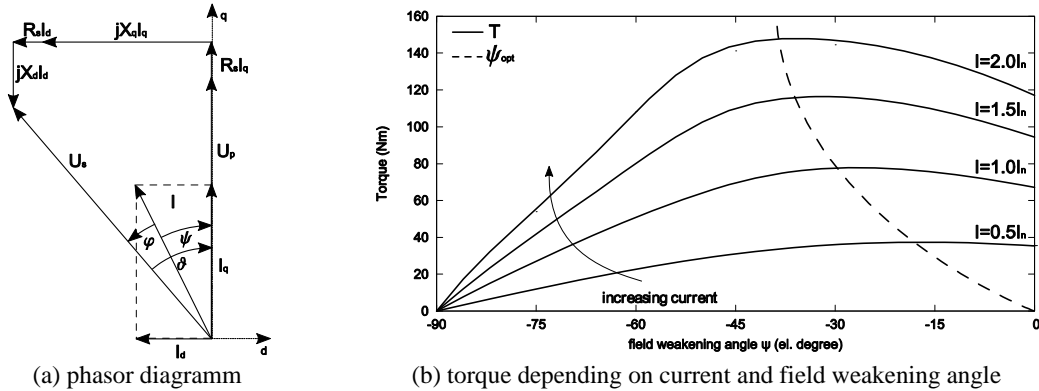


Fig. 2. The phasor diagram and torque characteristics of a synchronous machine with saliency.

Calculation methods

This section gives a detailed explanation and description of the applied loss-calculation methods for the iron losses in rotor- and stator lamination and the eddy-current losses in the permanent magnets.

Iron losses are computed by means of quasi-static numerical FE simulations and an improved post-processing formula based on the loss-separation principle [6]-[8], and that considers rotational hysteresis losses as well. The implemented formula is based on the loss separation principle in which the iron losses (P_{Fe}) are separated into hysteresis losses (P_h), eddy-current losses (P_{ec}) and excess losses (P_{ex}):

$$P_{Fe} = P_h + P_{ec} + P_{ex} \quad (1)$$

¹ Bundesministerium für Wirtschaft und Technologie (German Federal Ministry of Economics and Technology)

Eddy-current losses are calculated from the contributions of each harmonic as follows:

$$P_{ec} = k_{ec} \sum_{n=1}^{\infty} B_n^2 \cdot (n \cdot f)^2 \quad (2)$$

where B_n is the peak value of the magnetic flux density for the harmonic order n , and f the fundamental frequency. The constant k_{ec} depends on the sheet thickness, the mass density and the electric conductivity of the steel.

Excess losses are calculated in a similar way from the flux density of the different harmonics as:

$$P_{ex} = k_{ex} \sum_{n=1}^{\infty} B_n^{1.5} \cdot (n \cdot f)^{1.5} \quad (3)$$

Hysteresis losses depend on the frequency f and the peak value of the magnetic-flux density B and are determined by:

$$P_h = k_h [1 + c(r - 1)] B^2 \cdot f \quad (4)$$

The second term in (4) is a connection that accounts for rotational hysteresis losses [8]. It depends on an empirical factor r and the ratio $c = B_{min}/B_{max}$ that characterizes locally the locus of the B field. The material constants k_h and k_{ex} can be determined from the value of specific losses of the electrical steel at 1.5T and 50Hz ($p_{1.5T,50Hz}$) and at 1.0T and 50Hz ($p_{1.0T,50Hz}$).

The eddy-current density J_{ec} , in the permanent magnets, is calculated by the means of a transient 3D-FE approach, as described in [9]-[10]. The eddy-current density J_{ec} and the specific conductivity of the magnet material σ_{pm} are used to determine the eddy-current losses by integration over the magnet's volume V_{pm} :

$$P_{ec} = \int \frac{1}{\sigma_{pm}} \vec{J}_{ec}^2 dV_{pm} \quad (5)$$

Results of performed loss calculation with sinusoidal currents

The results of the loss calculations are presented and analyzed in this section. The iron losses are calculated for sinusoidal currents as a function of the rotational speed, the current peak value and the field-weakening angle ψ . Since iron losses increase monotonically with speed and frequency, as shown by (2)-(4), the losses against speed are not depicted here. In the following, loss calculations are done at a mechanical speed of $n=3000\text{min}^{-1}$.

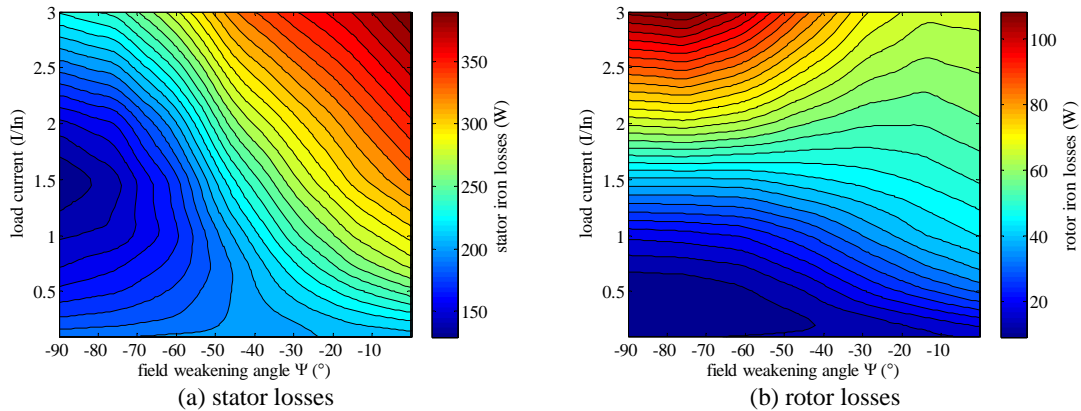
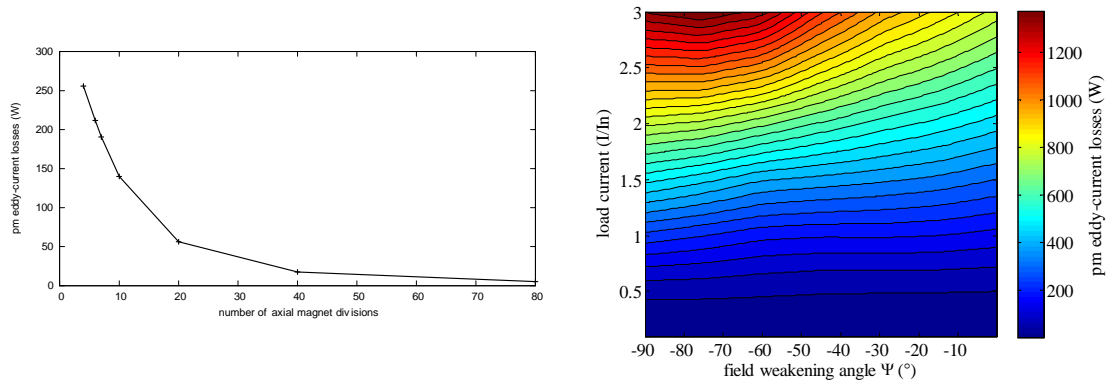


Fig. 3. Calculated iron losses depending on current peak value and field weakening angle.

Stator losses are reduced by increasing the field-weakening angle ($\psi \rightarrow -90^0$) and increased by increasing the load current at small field-weakening angles. However, at high field-weakening angles,

the stator losses are reduced first and increased then by increasing the load current, so a local minimum is formed (see Fig.3(a)).

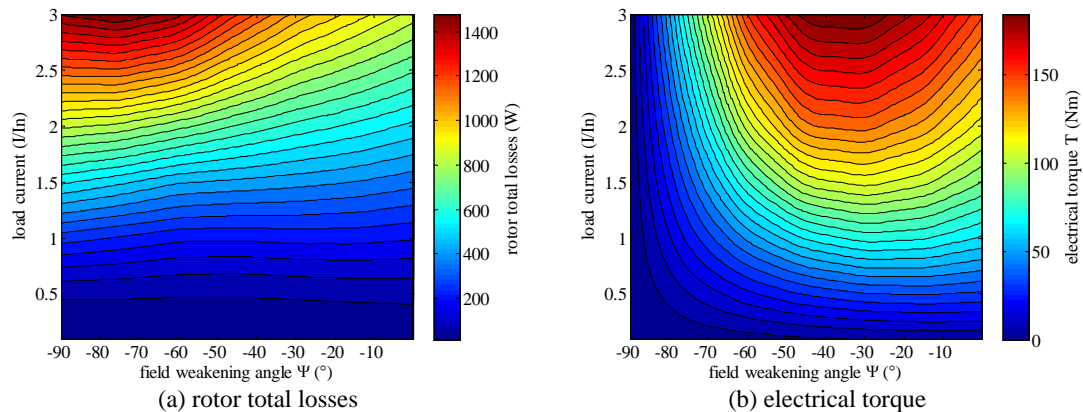
By contrast, rotor losses slightly decrease with growing field weakening at low currents, but at higher currents, they increase (see Fig.3(b)) when the field-weakening angle rises.



(a) depending on the axial segmentation (b) depending on current and field weakening angle
Fig. 4. Calculated eddy-current losses of permanent magnets.

The eddy-current losses in the permanent magnets are, in a first step, calculated with an axial segmentation of the magnets. If, as assumed here, the machine is operated with ideal sinusoidal currents, eddy-current losses are proportional to f^2 . Therefore, the loss calculations are performed at a mechanical speed of $n=3000\text{min}^{-1}$. Similar to the core lamination, the eddy-current losses decrease as the a the number of axial magnet division increases, see Fig.4(a). Since the relative loss difference between two segmentation numbers remains constant against all operation points (end effects are neglected, FE-model without end windings), the calculations were done with a segmentation number of 80 to keep the computational efforts and the 3D-FE model within reasonable limits. Due to feasibility reasons, the machine was prototyped with a axial magnet segmentation of 7 divisions.

The eddy-current losses in the magnets depending on the load current and field weakening angle (see Fig.4(b)) have similar characteristics to the rotor iron losses, i.e. they largely increase with rising field weakening and increasing load-current.



(a) rotor total losses (b) electrical torque
Fig. 5. Total rotor losses and resulting electrical torque depending on current and field weakening angle.

The total rotor losses are depicted in Fig.5(a). This shows that it is possible, especially at high currents, to lower the rotor losses but raise the stator losses (compare Fig.3(a)) by decreasing the field

weakening angle ($\psi \rightarrow 0^\circ$), i.e. the iron losses can be “moved” from rotor to the stator by an appropriate selection of the operation point. This is a great advantage because the permanent magnets are protected from heating. In addition, the heat, caused by the losses, can be dissipated more easily due to the stator’s water-cooling jacket.

The field-weakening angle is usually set by the controller depending on the maximum torque (see Fig.2(b) and Fig.5(b)) in the range of nominal speed, and depending on the limited terminal voltage in the range of field-weakening operation. But with respect to these results the losses in the permanent magnets should be considered in the design of the machine control as well, especially in overload operation.

Results of performed loss calculation depending on the current form

The losses, calculated so far, are caused by slot harmonics due to the permanent magnetic flux, the rotational speed and stator slots as well as the sinusoidal load current. But real currents in PWM-fed machines contain, besides the fundamental, higher harmonics causing additional losses. Moreover, the machine can be operated in the over-modulated region, or block-shaped voltages can be used. By these means it is possible to increase the speed range and improve the torque and thus the dynamic performances at high speeds. However, the resulting currents include high frequencies, too. Because the harmonic content has a great effect on the losses, the losses caused by three different current shapes are compared now: the sinusoidal, a block-shaped, and the real current at PWM supply, see Fig.6(a). The real current form was determined by a simulation containing the analytical IPMSM model, the PWM inverter (carrier frequency 20kHz) including power electronics and the machine controller. The amplitude of the block-shaped current is set in such a way, that the achieved average torque is equal to average torque resulting from the other current forms, see Fig.6(b). The constant output power assures a good comparability concerning losses and efficiency. The losses are calculated at $n=3000\text{min}^{-1}$ and $n=6000\text{min}^{-1}$. The machine is operated at nominal torque with the current $I=I_n$ and the field-weakening angle $\psi = \psi_{opt}$.

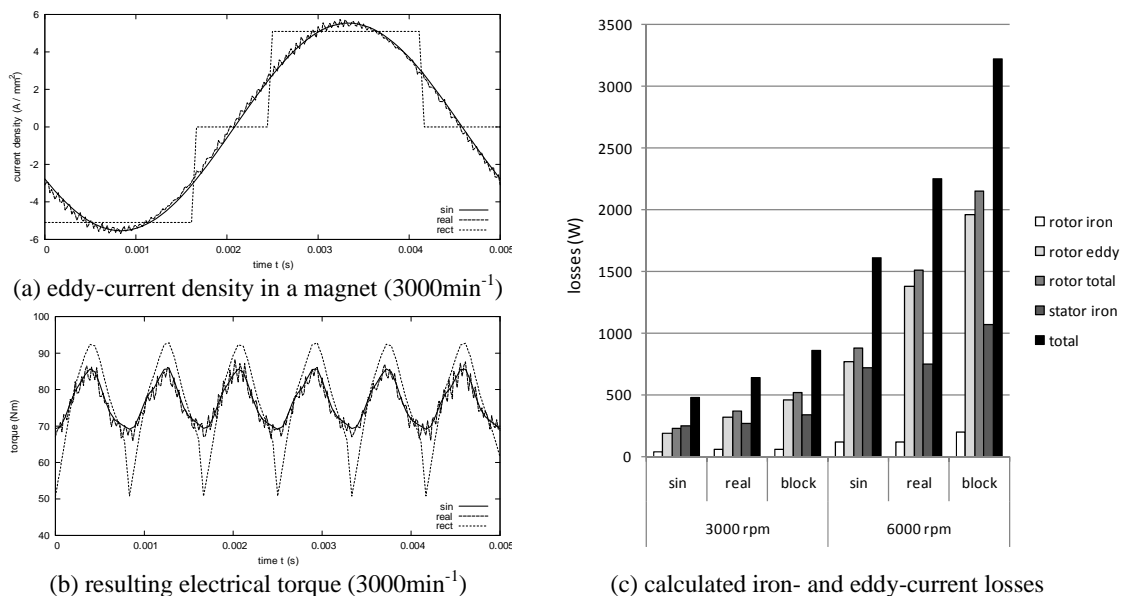


Fig. 6. Simulation results depending on the current form.

Compared to the operation with ideal sinusoidal currents, the stator-iron losses increase, depending on speed, by about 3%-7% with real currents and about 40% with block-shaped currents. The rotor-iron

losses rise by about 10%-50% (real currents) and about 60% (block shaped). The increase of the magnets' eddy-current losses is much higher, though. They increase, depending on speed again, by about 65%-80% (real currents) and about 140%-160% with block-shaped currents. The total (iron- and eddy-current) losses of the machine increase by about 35%-40% (real currents) and 80%-100% (block-shaped), compared to the losses at sinusoidal operation. All results are depicted in Fig.6(c). In view of these results, the control of the machine has to consider in particular the losses of the permanent magnets, particularly if the machine's speed range and dynamic performance is going to be increased and improved by the application of block-shaped currents.

Conclusion

In this paper the rotor- and stator-iron losses as well as the eddy-current losses in permanent magnets are calculated for different current values, field-weakening angles and rotational speeds. Since the harmonic content greatly affects the losses, the effect of block-shaped currents and real current forms of PWM-fed machines have also been studied in this paper.

It is shown that the field-weakening angle should not only be controlled depending on the maximum torque and limited terminal voltage, but also regarding the total rotor losses. For instance, the losses can be shifted from the rotor into the stator by decreasing the field-weakening angle. This protects the magnets from heating, and the heat, caused by the losses, can be dissipated more easily by means of a water-cooling jacket. The overload capacity of the machine and the thermal limits respectively can be improved this way.

Since the losses increase enormously with block-shaped currents, this must be considered if machine's speed range and dynamic performance is going to be increased and improved by the application of block-shaped currents.

References

- [1] A.M Hava, R.J. Kerkman, and T.A. Lipo, "Carrier-based PWM-VSI overmodulation region overmodulation strategies: analysis, comparison, and design", IEEE Trans. on Power Electronics, Vol.13 No.4, July, pp. 674-689, 1998.
- [2] J.S. Park, S.M. Jung, H.W. Kim, M.J. Youn, "Current control of PMSM in overmodulation region", Proc. of ICPE'07, p 1062-1065, 2008.
- [3] T. Weng, Y. Inoue, S. Morimoto, M. Sanada, "Expansion of operating range of sensorless PMSM drive by square-wave operation at high-speed", Proc. of 4th PCC-NAGOYA, p 308-313, 2007.
- [4] S. Morimoto, Y. Inoue, T.F. Weng, M. Sanada, "Position sensorless PMSM drive system including square-wave operation at high-speed", IEEE 42nd Annual Meeting, IAS, New Orleans, LA, p 676-682, 2007.
- [5] T. Finken, K. Hameyer, "Design and optimization of an IPMSM with fixed outer dimensions for application in HEVs", Proc. of International Electric Machines and Drives Conference, IEMDC, Miami, Florida, 2009.
- [6] G. Bertotti, „General properties of power losses in soft ferromagnetic materials”, IEEE Transactions on Magnetics, Vol. 24, No. 1 p. 621–630, January 1988.
- [7] G. Bertotti, A. Boglietti, M. Chiampi, D. Chiarabaglio, F. Fiorillo, M. Lazzari. „An improved estimation of iron losses in rotating electrical machines”. IEEE Transactions on Magnetics, Vol. 27, No. 6, p. 5007–5009, November 1991.
- [8] M. Herranz Gracia, E. Lange and K. Hameyer, "Numerical Calculation of Iron Losses in Electrical Machines with a modified Post-Processing Formula", in: Proc. of 16th COMPUMAG, Aachen, 2007.
- [9] C. Kaehler, G. Henneberger, „An Eddy-current computation in the claws of synchronous a claw-pole alternator in generator mode”. IEEE Transactions on Magnetics, Vol. 38, No. 2, p. 1201–1204, March 2002.
- [10] C. Kaehler, G. Henneberger, Eddy-current computation on a one pole-pitch model of a synchronous claw-pole alternator”. COMPEL - The International Journal for Computation and Mathematics in Electrical and Electronic Engineering, v 22, n 4, p 834-846, 2003.